A Novel Strategy to Intensify the Dissolution of Cellulose in Deep Eutectic Solvents by Partial Chemical Bonding

Yanhong Feng,[a] Guangliang Liu,[a] Hang Sun,[a] Chengcong Xu,[b] Bo Wu,[c] Canjun Huang,[d] and Bo Lei [a,]*

The relatively low solubility of cellulose in choline chloride-based deep eutectic solvents (DESs) restricts their practical application in the production industry. Here, cellulose was slightly oxidized into dialdehyde cellulose (DAC) at first, and then partial chemical bonding was introduced to intensify the dissolution process of cellulose in (choline chloride-resorcinol) DES. In this process, the solubility of cellulose in DES increased 10-fold, and the crystallinity of cellulose decreased over 24% while the oxidation level was lower than 20%. An intensified hydrogen bond network was revealed, which implied that cellulose components mainly acted as hydrogen bond donor after dissolution. A new class of DES containing cellulose was thus preliminarily established. The cellulose chains and the intensive hydrogen bond network also resulted in an increased viscosity and a conversion from Newtonian behavior to non-Newtonian behavior of dissolved samples. The phase transition behaviors of dissolved samples were gradually converted from crystallization to cool crystallization. The proposed and performed strategy is novel and scalable and will open a fresh perspective to achieve higher efficient dissolution of cellulose in DES and establish a new partially derivatized cellulose/DES system.

DOI: 10.15376/biores.17.3.4167-4185

Keywords: Cellulose; Deep eutectic solvents; Chemical bonding; Dissolution; Periodate oxidation

Contact information: a: Guangdong Provincial Key Laboratory of Technique and Equipment for Macromolecular Advanced Manufacturing; Key Laboratory of Polymer Processing Engineering, Ministry of Education; National Engineering Research Center of Novel Equipment for Polymer Processing, South China University of Technology, Guangzhou, 510640, PR China; b: Shaoguan Green & Low Carbon Materials Research Institute Co., Ltd., Shaoguan, 512000, PR China; and c: National Industrial Innovation Center of Polymer Materials Co., Ltd., Guangzhou, 510640, PR China; d: Guangdong Polytechnic of Water Resources and Electric Engineering, Guangzhou, 510640, PR China;
** Corresponding author: bo91lei@163.com*

INTRODUCTION

As one of the most abundant renewable biomass resources in nature, cellulose is typically considered as an ideal substitute for petroleum-based material due its biocompatibility, barrier properties, attractive appearance, non-toxicity, and low cost with the increasing demand for environmentally friendly and biodegradable products. However, cellulose is insoluble in most common solvents because of its high crystallinity and extensive intra- and intermolecular hydrogen bonds. To a great degree, this has limited the efficient conversion of this renewable resource into high value-added products (Djahedi *et al.* 2016).

Different cellulose solvents (DMAc(N,N-Dimethylacetamide)/LiCl, NMMO(N-methylmorpholine-N-oxide), molten salt hydrate, *etc.*) (Orelma *et al.* 2017; Han *et al.* 2019; Chen *et al.* 2020) were developed and studied in recent decades. However, the availability of these solvents applied to large-scale industrial work has been admittedly unacceptable. Increasing attention thus has been paid to look for more efficient, greener, safer, and cheaper solvents to dissolve cellulose for the sustainable development of society. For example, ionic liquids (ILs) and NaOH/Urea were shown to have a favorable capability for dissolving cellulose and exhibit remarkable potential in processing cellulose and exploiting high value-added products in industry (Cao *et al.* 2009; Li *et al.* 2015). Nonetheless, much more efforts should be made in the future to continue to reduce the solvents cost, simplify dissolution conditions and processes, and improve the availability of solvent to different cellulose materials.

Deep eutectic solvents (DESs) comprising of at least one hydrogen bond donor (HBD) and one hydrogen bond acceptor (HBA), emerged at the beginning of this century because of their low cost, negligible volatility, nonflammability, high conductivities, and other unusual solvent properties (Florindo *et al.* 2019). Recently, the applications of DESs in the dissolution and fractionation of lignocellulosic biomass have attracted increasing attention (Tang *et al.* 2017; Mamilla *et al.* 2019). It has been reported that DESs show good amounts of lignin solubility by regulating DESs components (Sosa *et al.* 2020; Yue *et al.* 2020), while they show significantly lower amounts of cellulose solubility (Francisco *et al.* 2012; Zhou and Liu 2014). Although a previous report has designed a molecular scissor based on reconstruction of hydrogen bonds by combining the DFT (density functional theory) theoretical calculations and experiment validation to achieve higher solubility of cellulose (between 10 and 17 wt%) in DESs, the main reason is that NMMO was used as the HBA (Luo *et al.* 2020). However, most previous studies on DESs for cellulose dissolution began with choline chloride (ChCl)-derived DESs because ChCl is the most popularly employed member for preparing DESs as a HBA, and the reported solubility of cellulose was usually lower than 1 wt% in these DESs, which has extremely hampered their practical application in the dissolution of cellulose (Chen *et al.* 2019). The prime reason is that hydrogen bond network in DESs results in fewer opportunities for interactions between solvent agents and cellulose and competition to react with chloride between protic –OH groups in the choline cation and hydrogen bonds in the cellulose.

There are many strategies to improve the solubility of cellulose in DES, such as increasing hydrogen bonding basicity (β) by regulating HBD and HBA (Abbasi *et al.* 2021), improving mass transfer processes using ultrasonic irradiation (Malaeke *et al.* 2018), and weakening hydrophobic interactions by adding a surfactant (Ren *et al.* 2016). Despite having a good practical effect, these strategies have resulted in a solubility of cellulose in DESs lower than 7 wt%, which was far from that in NMMO and ILs. Additionally, it was noteworthy that cellulose could form a DES because of the hydroxyl groups. At this point, a new class of DESs containing cellulose could be developed; however, this has yet to be reported with an available strategy (Tang *et al.* 2017; Chen *et al.* 2019). This is most likely attributed to a lack of effective principles or strategy for establishing a hydrogen bonding network between ChCl and cellulose.

In view of this situation, the current authors designed a partial chemical bonding intensified dissolution process of cellulose in DES based on phenol-aldehyde reaction. As detailed, cellulose was slightly oxidized first with sodium periodate to introduce aldehyde (Sirviö *et al.* 2011b), and subsequently reacted with phenolics in DES. Partial chemical bonding between cellulose and HBD was therefore achieved, and the slightly derivatized cellulose chain can be regarded as a new HBD. Finally, the solubility of cellulose in DES was thus significantly improved. This novel strategy would be promising in developing high value-added products from cellulose and has not been reported previously. In addition, according to previous studies, periodate oxidation of cellulose has a great potential for industrial development because the reaction conditions are mild and reagents are regenerative and recyclable (Koprivica *et al.* 2016; Dang *et al.* 2019). Moreover, phenol-aldehyde reaction has been widely used and can be controlled easily in industry (Xu *et al.* 2019). Therefore, this strategy also has great potential for large-scale industrialization. In this work, the current authors studied the dissolution behavior of cellulose with different oxidation levels and contents in DESs, and then investigated their physicochemical properties.

EXPERIMENTAL

Materials

Microcrystalline cellulose (MCC, ≤ 50 μm), used as raw cellulose, was purchased from Shanghai Aladdin Biochemical Technology Co., Ltd. (Shanghai, China). Choline chloride, resorcinol, sodium periodate, and ethanol were of analytical reagent grade and the deionized water was produced by an ultrapure water system. All chemical reagents were also purchased from Shanghai Aladdin Biochemical Technology Co., Ltd. (Shanghai, China).

Periodate Oxidation of MCC

Firstly, 10 g of MCC was suspended in 100 mL of distilled water in beakers. Periodate loadings of 0.3 and 0.6 g/g fibers were added into the suspension. The beakers were covered with aluminum foil to prevent photo-induced decomposition of the periodate.

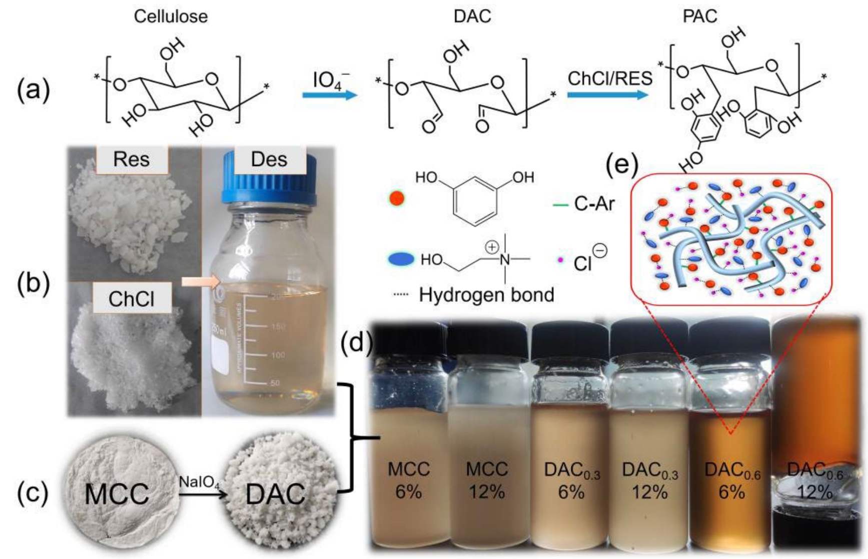

Fig. 1. (a) Chemical structure after reaction, (b) the synthesis of DES from ChCl and Res, (c) MCC and DAC samples, (d) dissolution of sample images, and (e) the hydrogen bonding network diagram of the dissolve sample

The reaction mixture was magnetically stirred at about 500 rpm and 45 °C for 10 h. Partially oxidized dialdehyde cellulose (DAC) was obtained (Fig. 1c) and named as DAC0.3 and DAC0.6. Microcrystalline cellulose underwent treatment at the same conditions without periodate as a reference. Microcrystalline cellulose, DAC0.3, and DAC0.6 were filtered and washed with distilled water and left without a drying treatment.

Preparation of DES

Choline chloride, resorcinol, and formic acid were mixed together in a molar ratio of 1:0.8:0.2. Then, the mixture was transferred to a sealed glass flask and heated to 80 °C, with constant stirring, for the time required until the formation of a clear liquid (Fig. 1b). The mixture was allowed to naturally cool to room temperature.

Dissolution of DAC in DES

For the dissolution of DAC in DES, 1.8 g and 3.6 g (abs.) of MCC, DAC0.3, and DAC0.6 were added in 30 g of DES. The mixtures were magnetically stirred at about 1000 rpm and 80 °C for 2 h. The resulting mixtures are presented in Fig. 1d, and named as DES/MCC-6%, DES/MCC-12%, DES/DAC0.3-6%, DES/DAC0.3-12%, DES/DAC0.6-6%, and DES/DAC0.6-12%, respectively. Most of the water in the wet MCC and DAC was removed by displacement with absolute ethanol before dissolving, and the remaining small amount of water, ethanol, and formic acid were removed by vacuum drying after the reaction.

Cellulose derivatives were regenerated before some characterization. The dissolved samples were dropped into ethanol and magnetically stirred for 1 h. Then, the obtained suspension was filtered and washed with ethanol to remove the remaining DES. The regenerated cellulose derivative was freeze-dried and named as the phenol-aldehyde reacted cellulose (PAC) (Fig. 1a).

Table 1. Abbreviation and Explanation of Sample Labels

	DAC	PAC	DES/MCC	DES/DAC
0.3	DAC0.3	PAC0.3		DES/DAC0.3-6%
0.6	DAC0.6	PAC0.6		DES/DAC0.6-12%
6%			DES/MCC-6%	DES/DAC0.6-6%
12%			DES/MCC12%	DES/DAC0.3-12%

Notes: 0.3 and 0.6 were the weight ratio of Periodate to MCC; 6% and 12% were the weight ratio of solute to solvent.

Characterization

Polarized light microscopy (POM)

A droplet of mixture was deposited on a microscope slide and sealed with a cover glass for observation. Optical characterization of the dissolved samples was completed using POM with an Olympus transmission microscope (Olympus, Tokyo, Japan) coupled with a Leica digital camera and Leica Application Suite Software (Leica Camera, Inc., version 3.4.2. 18368,, Allendale, NJ, USA).

Fourier transform infrared spectrometry (FTIR)

The FTIR spectra of different samples were recorded using a Nicolet 6700 FTIR spectrometer (Thermo Scientific, Waltham, MA, USA) equipped with a diamond crystal as ATR (attenuated total reflectance) element in a spectral range of 400 to 4000 cm^{-1} with a resolution of 4 cm^{-1} resolution by accumulating 32 scans.

Differential scanning calorimetry (DSC) analysis

Thermal characterization was completed using DSC (Netzsch 204F1, Netzsch GmbH & Co., Sleb, Germany). Approximately 10 mg of the samples were placed in the aluminum crucible with cover. The runs were conducted in three stages: i) heating from 30 °C to 105 °C at a heating rate of 10 °C/min, holding this temperature for 10 min to eliminate the effect of trace water; ii) cooling from 105 °C to -45 °C at 3 °C/min, holding this temperature for 5 min; and iii) heating from -45 °C to 105 °C at 3 °C/min under a nitrogen atmosphere fed with a flow rate of 50 mL/min.

X-ray diffraction (XRD) analysis

The crystallinity was determined by wide-angle X-ray diffraction (WAXD) using a Bruker D8 Advance X-ray diffractometer (Bruker Daltonics GmbH & Co., Bremen, Germany). The scattering angle range was 5 to 40°, the scanning speed was 4°/min, and the 2θ step interval was 0.02°. The XRD data were analyzed by calculating the ratio between the diffraction of the (002) lattice peak at about 22.5°, and the minimum was found between the (002) and (101) lattice peaks at approximately 18.5°, commonly referred to as the crystallinity index (CrI).

Rheological characterization

Viscosity analyses of the dissolved samples were characterized by steady rheological measurements on a MCR 302 modular compact rheometer (Anton Paar Austria GmbH, Graz, Austria) fitted with a parallel plate geometry with 50 mm diameter and a gap of 0.1 mm. The viscosities were measured in the range of shear rate from 0.1 to 700 s^{-1} at constant temperature of 25 °C in triplicates. The flow curves were obtained using RheoPlus software (Anton Paar, RheoCompass1.12, Austria GmbH, Graz, Austria).

Aldehyde content analysis

The aldehyde content of DAC was determined by the oxime reaction between the aldehyde groups and $NH_2OH \cdot HCl$. The $NH_2OH \cdot HCl$ solution (25 mL of 0.25 M) used here was adjusted to pH 4. The never-dried periodate oxidized cellulose (approx. 0.1 g abs.) was then added to the solution and stirred at room temperature for 4 h. Finally, the reaction mixture was titrated back to pH 4 using standardized 0.1 M sodium hydroxide. The aldehyde content of the oxidized samples was calculated according to the amount of sodium hydroxide. Each reaction with $NH_2OH \cdot HCl$ was performed in triplicate (Larsson and Wågberg 2016).

Determination of solubility

Then, 0.6 g, 1.2 g, and 1.8 g (abs.) of MCC, DAC0.3, and DAC0.6 were added to 30 g of DES, respectively. The dissolved process is shown in Fig. 1. Each dissolved sample was divided into three points and centrifuged at 10000 rpm for 10 min. Then, 3 g of supernatant were dropped into ethanol and magnetically stirred for 1 h. The regenerated cellulose derivatives were freeze-dried and weighed. The solubility of cellulose can be calculated based on the sampling ratio. It should be noted that higher amounts of DAC would result in higher viscosity of dissolved samples and cannot achieve the separation of the dissolved part and undissolved part, which was thus not investigated in this work.

RESULTS AND DISCUSSION

Periodate Oxidation and Phenol-aldehyde Reaction

Aldehyde content was measured to provide insight regarding the periodate oxidation of MCC and phenol-aldehyde reaction between DAC and DES, as shown in Fig. 2a. The aldehyde content of DAC0.3 and DAC0.6 was 1.05 mmol/g and 2.14 mmol/g respectively, which corresponded to the oxidation levels of 8.5% and 17.3%. And then, the yields of DAC0.3 and DAC0.6 obtained were 97.5% and 96.2% respectively, which were notably high at the lower oxidation level. Inspired by previous reports (Lucia *et al*. 2019), the current authors performed the periodate oxidation with a relatively high-consistency cellulose (MCC/water ratio of 1:10) and the low amounts of periodate for achieving resources-saving production of DAC. In this work, the relatively lower oxidation level could avoid the decomposition of cellulose as soon as possible (Sirviö *et al.* 2011a), but resulted in a remarkable decrease in CrI of DAC (Fig. 4b).

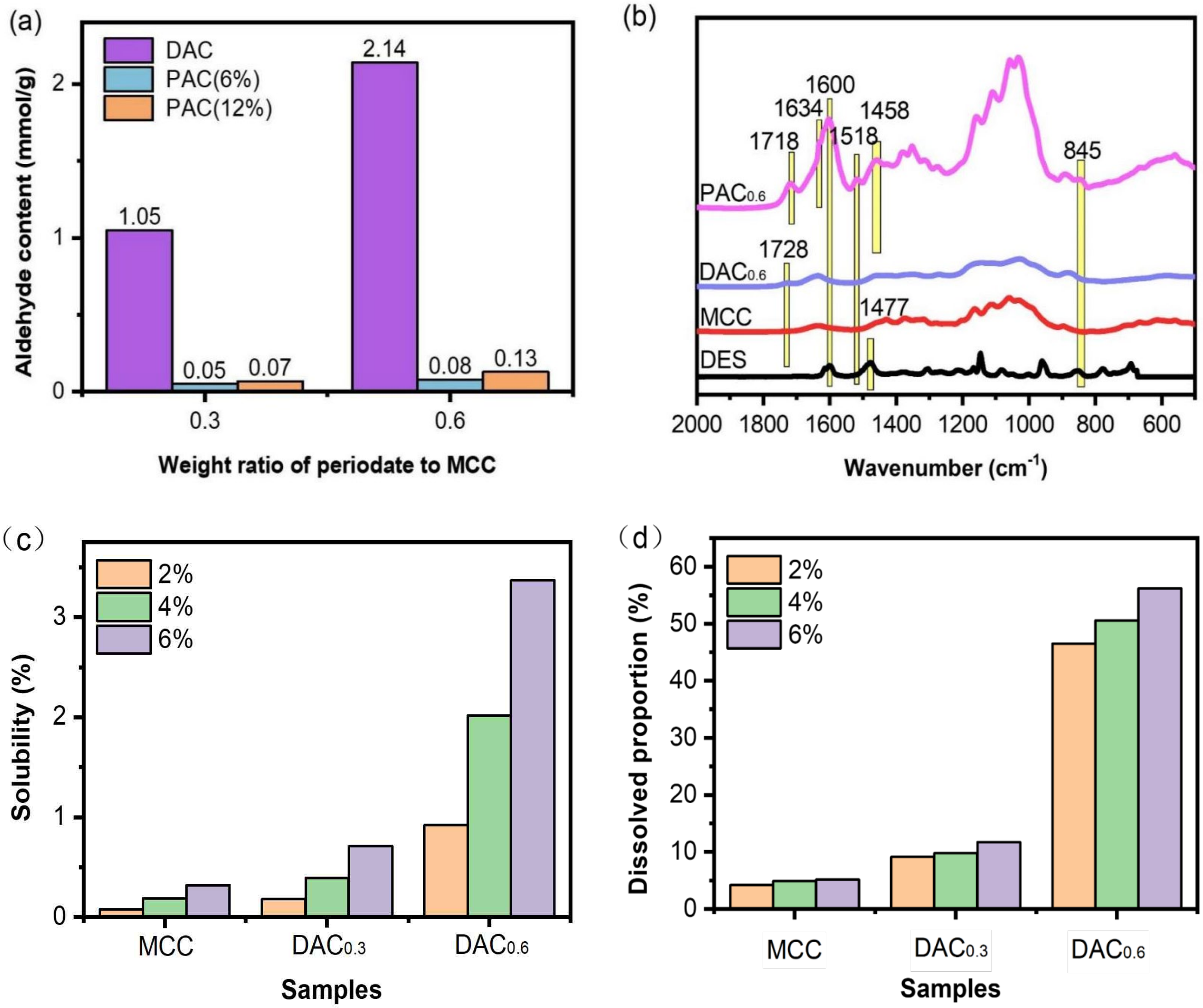

Fig. 2. (a) the aldehyde content of DAC and PAC, (b) The FTIR spectra of DES, MCC, DAC0.6, and PAC0.6, (c) the solubility of cellulose in DES at different amounts of MCC or DAC, and (d) the dissolved proportion of MCC and DAC

The aldehyde contents of PAC are also presented in Fig. 2a, which indicated that the aldehyde contents were decreased noticeably after phenol-aldehyde reaction. This implied that most of the aldehyde groups (> 90%) participated in the reaction. A small amount of residual aldehyde is most likely because gelation of DAC particles might occur during the dissolution process of cellulose (Cai and Zhang 2006) and hampered the reaction between resorcinol and aldehyde. A slightly higher aldehyde content at a higher weight ratio of DAC to DES (12%) also validated this reason. Moreover, there were steric-hindrance effects for this reaction between two resorcinol groups and DAC, which could also result in a little aldehyde without being involved in this reaction. These results were consistent with a previous study, in which the degree of substitution of cellulose during esterification was relatively lower when using diphenyl chlorophosphate as a substituent group (Xiao *et al.* 2014).

Phenol-aldehyde reaction was confirmed by FTIR spectrum presented in Fig. 2b. The band observed at 1728 cm^{-1} appeared in DAC0.6 and was attributed to C=O vibrations of aldehyde, while it almost disappeared in PAC0.6. The band at 1718 cm^{-1} may be related to C=O on the ester group formed by the reaction of formic acid. It should be noted that the benzene ring skeleton vibration signals appeared at 1600, 1518, and 1458 cm^{-1}. In addition, the signal of 1, 3, 5 substituted benzene ring also appeared at 845 cm^{-1} of the band. This indicated that phenols reacted with DAC and were successfully grafted on the molecular chain. It was noteworthy that a new band related to C=O appeared at 1634 cm^{-1} in PAC0.6. This is because phenolic compounds can be oxidized to quinones. At the same time, it should be noted that the band at 1477 cm^{-1} also appeared in DESs, which corresponded to CH_2 in ChCl, but it was not observed in the PAC spectrum. This indicated that DAC did not react with ChCl in DES.

The synthesis of phenolic resin was divided into two stages: addition reaction and polycondensation, and the products usually were affected by pH and the molar ratio of phenol to aldehyde. Resorcinol-formaldehyde polycondensation has been demonstrated in previous reported studies in a DES system (Gutiérrez *et al.* 2010), which revealed the feasibility of phenol-aldehyde reaction. However, the difference in the reaction was that the aldehyde groups were scattered at the cellulose molecular chains, and then the dissolved cellulose molecular chains caused a higher viscosity. Therefore, the polycondensation of phenol and aldehyde was extremely difficult, while addition reaction dominated. The addition reaction usually occurred in the ortho- and para-positions of the phenolic hydroxyl group, as shown in Fig. 1b. It should also be noted that ChCl/RES DES provided a weakly acidic environment, which could catalyze the phenol-aldehyde reaction. However, the more detailed information about the chemical structure of PAC and the reaction kinetics of addition reaction and polycondensation during phenol-aldehyde reaction are still unclear and require much more systematic and in-depth research.

The solubility of cellulose in DES with different oxidation levels and dosages is presented in Fig. 2c. It can be observed that the solubility of MCC in DES was less than 1%, which was noticeably lower than 6%, as reported in a previous study. The reason is that the MCC with higher crystallinity (> 80%) was used as raw material in this work. Furthermore, ultrasonic irradiation was not used for improving the mass transfer (Malaeke *et al.* 2018). The solubility of DAC0.6-6% was 3.37%. It increased approximately 10 fold compared to MCC-6%, which showed that partial chemical bonding remarkably intensified the dissolution of cellulose. Moreover, the dissolved proportion of DAC0.3 was relatively stable based on its dosages as well as MCC. However, the dissolved proportion of DAC0.6 was slightly increased as its dosage increased. This was most likely because much more dissolved cellulose chains formed an entanglement network and resulted in higher viscosity, which could make the little undissolved micro-nano crystalline region be retained in the supernatant after centrifugation.

Microstructure of MCC or DAC during Dissolution

The microstructure of MCC, DAC, and their dissolved samples were investigated using POM, as shown in Fig. 3. The MCC crystalline structure can be clearly observed in Fig. 3a. Despite periodate oxidizing with periodate loadings of 0.6 g/g fibers, most of the crystalline structure remained (Fig. 4b). However, DAC0.6 was easier to aggregate due to the increase of amorphous components and the interaction of DAC molecules (Lopez-Sanchez *et al.* 2017). This is shown in Fig. 3c, in which cellulose crystalline (light color) is wrapped with amorphous components (shadows). It can be observed that there was a certain amount of crystalline structure in Fig. 3d, which also confirmed the extremely lower solubility of cellulose in DES.

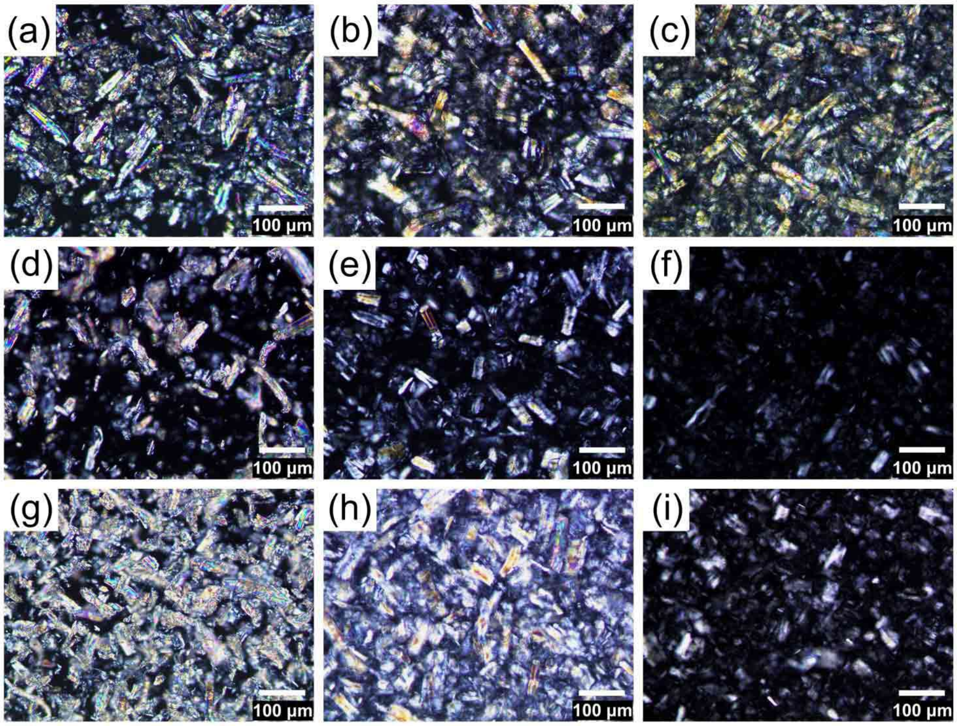

Fig. 3. POM images of: (a through c) MCC, DAC0.3, and DAC0.6 in water, (d through f) DES/MCC-6%, DES/ DAC0.3-6%, and DES/DAC0.6-6%, and (g through i) DES/MCC-12%, DES/ DAC0.3-12%, and DES/DAC0.6-12%, respectively

The crystalline structure in DESs was noticeably decreased after the introduction of aldehyde. There is a sparse luminous region distributed in Fig. 3f, which indicated that the majority of the crystalline structure was destroyed. Then, the interference color gradually became single and bleak, which represented the weakly birefringent resulting from the destruction of cellulose crystalline. This feature can also be confirmed by a remarkable decrease of the CrI (Fig. 4b.) from 40.6% (DAC0.6) to 16.2% (PAC0.6-6%). However, this also implied that little crystalline region remained. The most plausible reason is that the introduction of aromatic ring was more destructive around the crystalline region, while it was less destructive to the distant crystalline region, as presented in Fig. 4c (black dotted arrow). This demonstrated that DAC can almost entirely dissolve in DES at a higher oxidation level, as shown in Fig. S1. Furthermore, compared to Fig. 3f (DES/DAC0.6-6%), a little more luminous region was observed in Fig. 3i (DES/DAC0.6-12%) because the higher viscosity would make the mass transfer difficult, thus further hampering the destruction of crystalline cellulose. It should be noted that the remaining crystalline region can play an important role, for example, as a reinforcement phase in all-cellulose composites, as reported in previous literature (Baghaei and Skrifvars 2020).

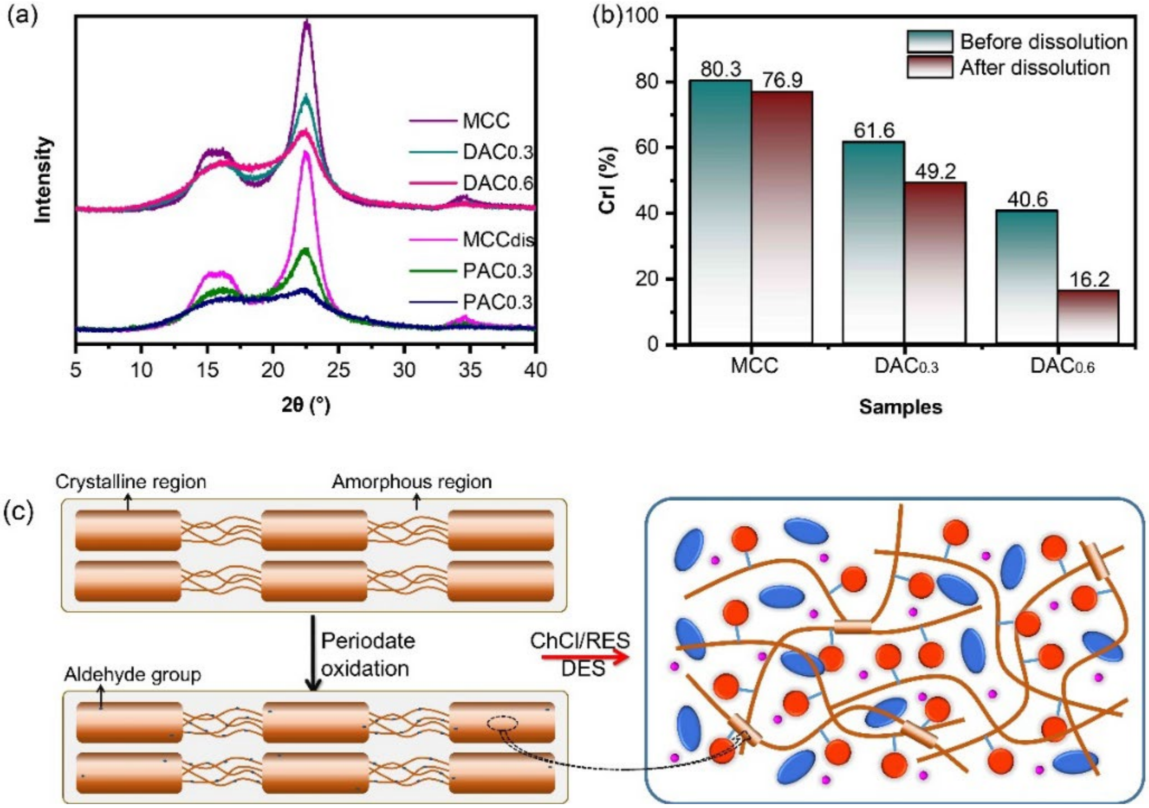

Fig. 4. The XRD spectra (a) and CrI (b) of MCC, DAC, and their regenerated products from dissolved samples, and (c) schematic diagram of the change of the aggregated structure

According to the diffraction patterns and CrI results (Fig. 4ab), the crystal type of cellulose was not changed, while the CrI of samples after dissolution decreased. Then, the differences in CrI between DAC and PAC increased as the oxidation level increased, which implied that much more crystalline cellulose region was destroyed at a higher oxidation level. This mechanism of this phenomenon was that the insertion of the aromatic ring into cellulose chains promoted the separation of cellulose chains and increased the distance between the cellulose chains. These improved the mass transfer of DES and made the hydrogen bond network between cellulose and DES reconstruct easier, as presented in Fig. 4c. It is widely accepted that DESs have poor solubility of cellulose due to their weaker capability in disrupting the inherent hydrogen bond network of cellulose, especially for crystalline cellulose (Zhang *et al.* 2020). However, in this work, this process was noticeably improved by insertion of the aromatic ring based on partial chemical bonding, and thus resulted in a remarkable increased solubility of cellulose in DES. The authors also investigated the dissolution of DAC in ChCl/glycerol and found that the dissolution process was not improved, which also implied the critical role of partial chemical bonding.

Hydrogen Bond Network between DAC and DES

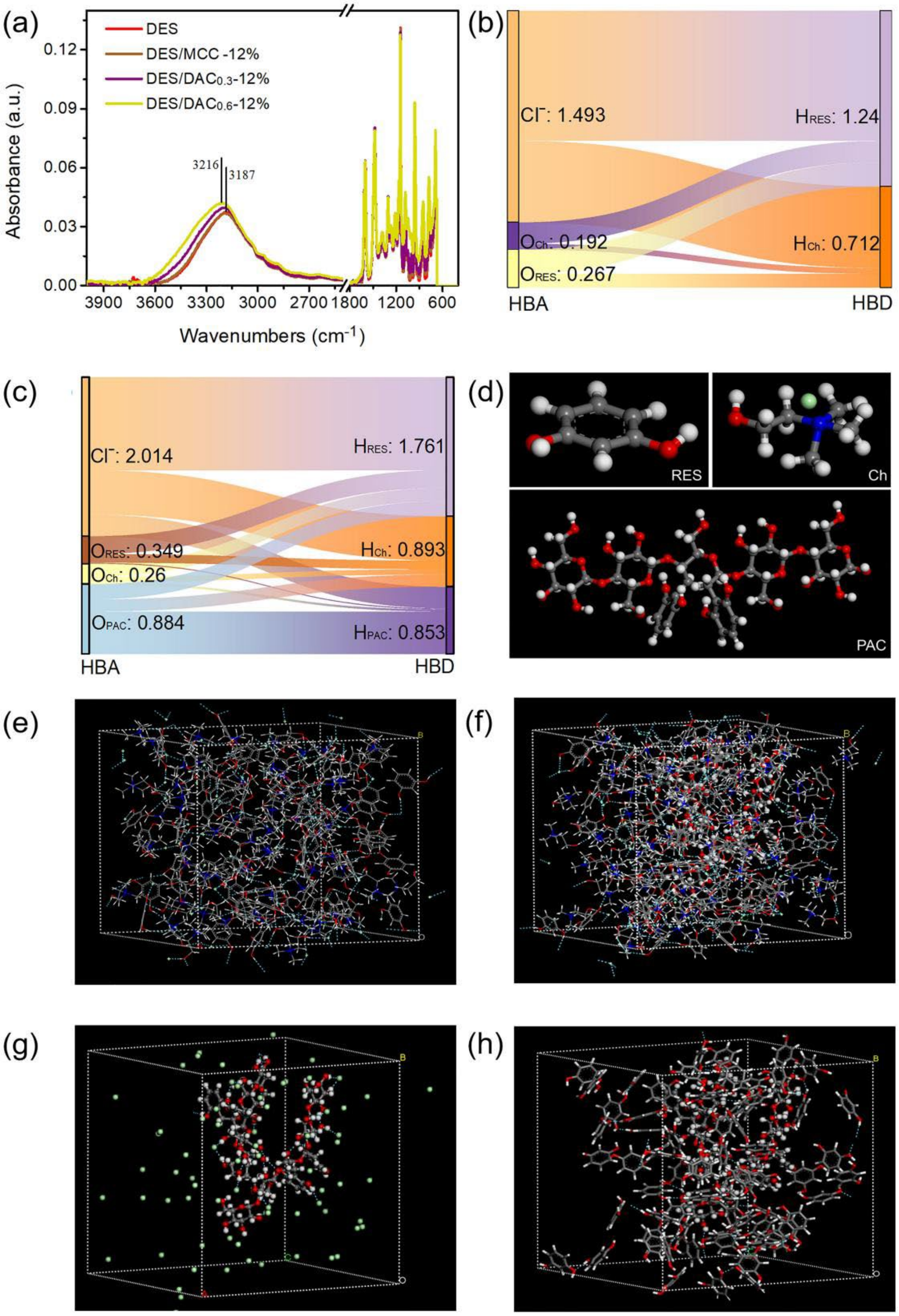

Fig. 5. (a) The FTIR spectra of dissolved samples, (b) the Sankey diagram visualizing the topology of the hydrogen band network for the DES and (c) DAC solution in DES, (d) the molecular model of RES, Ch, and PAC, and (e) the hydrogen bond network in molecular model for the DES, (f) DAC solution in DES, (g) the hydrogen bond network in molecular model between Cl^- and PAC, and (h) the hydrogen bond network in molecular model between resorcinol and PAC.

The hydrogen bond networks of DES and the dissolved samples were investigated to understand the dissolution mechanism, as shown in Fig. 5. The FTIR spectra of DES and the dissolved samples are presented in Fig. 5a. A typical band attributed to the stretching vibration of –OH groups shifted from 3187 cm^{-1} to 3216 cm^{-1} and broadened as the oxidation level increased. It was noteworthy that this phenomenon mainly occurred in DES/DAC instead of DES/MCC, which suggested that the –OH group in the cellulose chain corresponding to higher wavenumbers was introduced into DES and formed hydrogen bond networks (Oh *et al.* 2005). In this dissolved system, the Cl atom and O atom used as HBA attracted H atom in the HBD. After dissolution of cellulose, different O atoms and H atoms were introduced into the dissolved system. However, it has been reported that mainly only the O atom and H atom in primary and secondary hydroxyl groups participated in the formation of hydrogen bond (Brehm *et al.* 2020).

To explain the changes of hydrogen bond more clearly, the authors examined the types of hydrogen bond and their amounts according to molecular simulation, as presented in Table S1 and Table S2. It was noteworthy that a noticeable increase of hydrogen bond between Cl atom and –OH groups in RES (resorcinol) and cellulose (Cl···O–H) was observed because of higher electronegativity of Cl atom (Benabid *et al.* 2019), which confirmed the intensive interaction enhanced by partial chemical bonding. In addition, –OH groups in cellulose as HBD can form the hydrogen bond with O atom in –OH groups of RES and choline cation. This showed that cellulose mainly acted as HBD in the hydrogen bond network of the dissolved system. Only a few O atoms as HBA formed hydrogen bond with H atom in –OH groups of RES and choline cation. According to the examined values, the authors established the Sankey diagrams (Fig. 2bc) to visualize the topology of the hydrogen bond network (Brehm *et al.* 2020), which showed the formation of a more complex hydrogen bond network between cellulose and DES, as also presented in Fig. 1e. Additionally, a new class of DESs containing partially derivatized cellulose was preliminarily developed. Admittedly, much more efforts should be made to investigate the structure and configuration of PAC with the aim of further optimizing the hydrogen bond network, which is essential for interpreting and regulating their physicochemical properties.

Flow Curves of MCC and DAC Dissolved Samples

The rheological properties of cellulose solutions are crucial to process and develop their materials and products. As presented in Fig. 6, DES kept constant viscosity over the whole shear rate range applied, which exhibited typically Newtonian behavior (Altamash *et al.* 2017). It was noteworthy that there were barely changes in viscosity and Newtonian behavior for the mixture of DES and MCC. Furthermore, the beginning of shear thinning was observed (non-Newtonian behavior) for the DES/DAC0.3-6% under a shear rate domain of 0.1 to 1 S^{-1}. However, the viscosity of DES/DAC0.3-6% was still independent of shear rate within the range of 1 to 700 S^{-1}. Moreover, with the increase of the contents and the oxidation level of DAC in DES, the non-Newtonian behavior became more distinct, and the viscosity was increased noticeably. More importantly, the dependence of viscosity on high shear rate was gradually increased. Especially for DES/DAC0.6-12%, the non-Newtonian behavior occurred over the whole shear rate range applied, and the viscosity decreased linearly with the increase of shear rate.

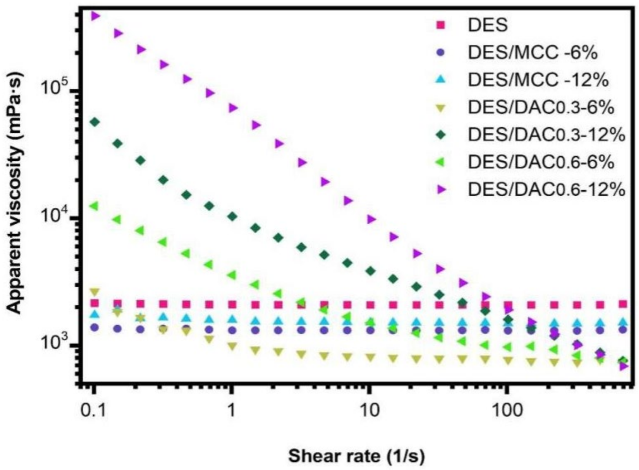

Fig. 6. Steady-state shear viscosity of dissolved samples of MCC and DAC in DES

It has been reported that DESs usually exhibit high viscosity at room temperature because of the prevailing hydrogen bond network between the components, which results in a limited mobility of free species with the DES (Elhamarnah *et al.* 2019; Fan *et al.* 2021). In this work, comparing the viscosity of DES, DES/MCC, and DES/DAC0.3-6%, it can be concluded that the addition of MCC particles under a relatively low proportion range had a negligible impact on their viscosity and Newtonian behavior. Therefore, the increasing viscosity and the exhibiting of non-Newtonian behavior were attributed to the materials in the dissolved state. This would form a new hydrogen bond network between polymer molecular chain and DES. The mixtures of DES and DAC were thus converted into a typical polymer solution. The shear-thinning behavior in many classic polymer melts or solutions is generally considered to be induced by the rearrangement and orientation of macromolecular chains along the shear direction (Lu *et al.* 2015). With increasing of oxidation level and additive amount of DAC, the materials in the dissolved state was increased, and thus resulted in a higher apparent viscosity and a higher dependence of viscosity to shear rate. This further demonstrated the fact that the increasing solubility of cellulose in DES was achieved by partial chemical bonding. The results also suggested that the newly formed DES containing partially derivatized cellulose showed an obviously distinct rheological behavior compared to pure DES.

Melting and Crystallization Behavior

The dissolved samples were characterized by DSC to determine the existence of phase transitions, including melting and crystallization behavior. The DSC of DES was dominated by the presence of a sharp exothermic peak at −9.4 °C with a Δ*H* of −73.78 J/g in the cooling curve. However, as observed for the DES/MCC-6% and DES/MCC −12%, the sharp exothermic peak gradually shifted to a lower temperature of −11 °C and −17 °C, with a Δ*H* of −64.93 J/g and −49.34 J/g, respectively. The results from the DSC cooling curve (Fig. 7a) indicated that the addition of MCC would slightly hinder the crystallization of DES, because the presence of MCC particle in DES inhibited the formation efficiency of eutectic system between ChCl and RES. The endothermic transitions that ensue were assigned to the melting of the crystalline structures. It can be observed that two endothermic peaks between 10 and 40 °C were formed in all samples, which was attributed to the solid (at approximately 17.7 °C) and solid–liquids (at approximately 29.1 °C) transition (Aroso *et al.* 2016).

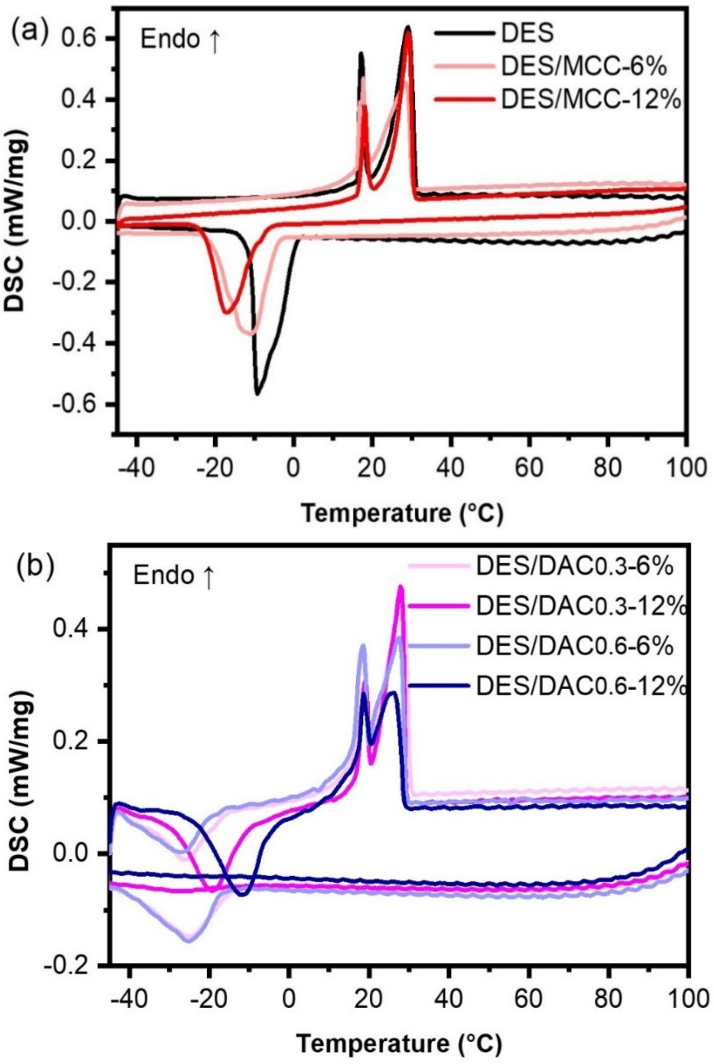

Fig. 7. The DSC thermograms (cooling and heating step) of (a) DES, DES/MCC-6%, and DES/MCC-12%, and (b) DES/DAC0.3-6%, DES/DAC0.3-12%, DES/DAC0.6-6%, and DES/DAC0.6-12%

It was noteworthy that the two exothermic peaks of DES/DAC0.3-6% and DES/DAC0.6-6% appeared at approximately −25 °C (< −17 °C) in cooling curves and heating curves, which corresponded to crystallization during the cooling step and cold crystallization during the heating steps. The reason was that there was the interaction between the cellulose molecular chain and the DES molecules, which inhibited the migration and arrangement efficiency of the DES molecules during the cooling process, and was difficult to crystallize completely. However, during the reheating, the non-crystallized DES molecules gained energy. DES molecules can migrate easily and further arranged in an orderly manner, and formed a cold crystallization. In addition, the crystallization in the cooling step disappeared obviously, especially in the thermograms of DES/DAC 0.6-12%, which was also due to the hindering of cellulose molecular chains that affected the crystallization behavior of DES (Aroso *et al.* 2017). These results suggested that the dissolved cellulose chains had a much more noticeable impact on the phase transitions of DES compared to undissolved MCC particles. This was mainly attributed to the formation of hydrogen bond network between DES and cellulose chains, as confirmed by FTIR and molecular simulation (Fig. 5). In general, the phase transitions of DES were closely related to its hydrogen bond network, however, it changed due to the introduction of cellulose chains (Francisco *et al.* 2012). Therefore, the ordered eutectic structure was more difficult to form, especially when many more partially derivatized cellulose chains existed in DES.

In addition, an exothermal cold crystallization transition of DES/DAC0.6-12% appeared at approximately −12 °C, which was higher than approximately −20 °C of DES/DAC0.3-12%. This can also suggest that the hydrogen bond between cellulose chain and DES affected the phase transitions of DES. It was also noteworthy that the cold crystallization temperature was gradually close to the melting temperature, which might eventually turn into the glass transition of the new class of DESs when containing many more cellulose chains. This will be favorable to the development of new cellulose-based bioplastics. However, with this goal, a great deal of research work for improving mass transfer and achieving higher solubility of cellulose in DES needs to be conducted in the future.

CONCLUSIONS

1. A novel and scalable strategy for achieving higher solubility of cellulose in deep eutectic solvents (DES) and establishing a new class of DES containing partially derivatized cellulose was proposed and performed. Dialdehyde cellulose with a low oxidation level reacted with phenol and formed new chemical bonds, which thus intensified the destruction of cellulose crystalline region and resulted in higher solubility of cellulose in DES.
2. A new hydrogen bond network between DES and partially derivatized cellulose was rebuilt, and the amounts of Cl···O–H hydrogen bond were noticeably increased, which revealed the extensive interaction between the Cl atom and partially derivatized cellulose. The dissolved partially derivatized cellulose chains resulted in a remarkable increase in the viscosity of the dissolved samples and made them show non-Newtonian behavior.
3. And then, the reconstruction of hydrogen bond between DES and partially derivatized cellulose showed inhibitory effects on crystallization. Cool crystallization gradually appeared, and the crystallization temperature was gradually increased to close to the melting temperature.
4. This study developed a new class of the partially derivatized cellulose/DES solution system; their physicochemical properties also implied a promising practical application in cellulose processing. Subsequently, a great deal of work needs to be done under the efficient mass transfer process, such as ultrasonic irradiation and high mechanical shear, to achieve higher solubility of cellulose and develop high value-added materials.

ACKNOWLEDGMENTS

This work was supported by the National Natural Science Foundation of China (Grant Nos. 51873073), the Science and Technology Planning Project of Guangzhou city (Grant No. 202002030350), Guangdong General University Characteristic Innovation Project (Higher Vocational College 2019GKTSCX051), and the Natural Science Foundation of Guangdong Province, China (Grant No. 2022A1515011561).

REFERENCES CITED

Abbasi, N. M., Farooq, M. Q., and Anderson, J. L. (2021). "Modulating solvation interactions of deep eutectic solvents formed by ammonium salts and carboxylic acids through varying the molar ratio of hydrogen bond donor and acceptor," *Journal of Chromatography A* 1643, article ID 462011. DOI: 10.1016/j.chroma.2021.462011

Altamash, T., Nasser, M. S., Elhamarnah, Y., Magzoub, M., Ullah, R., Anaya, B., Aparicio, S., and Atilhan, M. (2017). "Gas solubility and rheological behavior of natural deep eutectic solvents (NADES) *via* combined experimental and molecular simulation techniques," *ChemistrySelect* 2(24), 7278-7295. DOI: 10.1002/slct.201701223

Aroso, I. M., Paiva, A., Reis, R. L., and Duarte, A. R. C. (2017). "Natural deep eutectic solvents from choline chloride and betaine – Physicochemical properties," *Journal of Molecular Liquids* 241, 654-661. DOI: 10.1016/j.molliq.2017.06.051

Aroso, I. M., Silva, J. C., Mano, F., Ferreira, A. S. D., Dionísio, M., Sá-Nogueira, I., Barreiros, S., Reis, R. L., Paiva, A., and Duarte, A. R. C. (2016). "Dissolution enhancement of active pharmaceutical ingredients by therapeutic deep eutectic systems," *European Journal of Pharmaceutics and Biopharmaceutics* 98, 57-66. DOI: 10.1016/j.ejpb.2015.11.002

Baghaei, B., and Skrifvars, M. (2020). "All-cellulose composites: A review of recent studies on structure, properties and applications," *Molecules* 25(12), article no. 2836. DOI: 10.3390/molecules25122836

Benabid, S., Benguerba, Y., AlNashef, I. M., and Haddaoui, N. (2019). "Theoretical study of physicochemical properties of selected ammonium salt-based deep eutectic solvents," *Journal of Molecular Liquids* 285, 38-46. DOI: 10.1016/j.molliq.2019.04.052

Brehm, M., Radicke, J., Pulst, M., Shaabani, F., Sebastiani, D., and Kressler, J. (2020). "Dissolving cellulose in 1,2,3-triazolium-and imidazolium-based ionic liquids with aromatic anions," *Molecules* 25(15), article ID 3539. DOI: 10.3390/molecules25153539

Cai, J., and Zhang, L. (2006). "Unique gelation behavior of cellulose in NaOH/urea aqueous solution," *Biomacromolecules* 7(1), 183-189. DOI: 10.1021/bm0505585

Cao, Y., Wu, J. V., Zhang, J., Li, H., Zhang, Y., and He, J. (2009). "Room temperature ionic liquids (RTILs): A new and versatile platform for cellulose processing and derivatization," *Chemical Engineering Journal* 147(1), 13-21. DOI: 10.1016/j.cej.2008.11.011

Chen, Y., Yu, H., and Li, Y. (2020). "Highly efficient and superfast cellulose dissolution by green chloride salts and its dissolution mechanism," *ACS Sustainable Chemistry and Engineering* 8(50), 18446-18454. DOI: 10.1021/acssuschemeng.0c05788

Chen, Y., Zhang, X., You, T., and Xu, F. (2019). “Deep eutectic solvents (DESs) for cellulose dissolution: A mini-review,” *Cellulose* 26(1), 205-213. DOI: 10.1007/s10570-018-2130-7

Dang, X., Liu, P., Yang, M., Deng, H., Shan, Z., and Zhen, W. (2019). “Production and characterization of dialdehyde cellulose through green and sustainable approach,” *Cellulose* 26(18), 9503-9515. DOI: 10.1007/s10570-019-02747-9

Djahedi, C., Bergenstråhle-Wohlert, M., Berglund, L. A., and Wohlert, J. (2016). “Role of hydrogen bonding in cellulose deformation: The leverage effect analyzed by molecular modeling,” *Cellulose* 23(4), 2315-2323. DOI: 10.1007/s10570-016-0968-0

Elhamarnah, Y. A., Nasser, M. S., Qiblawey, H., Benamor, A., Atilhan, M., and Aparicio, S. (2019). “A comprehensive review on the rheological behavior of imidazolium based ionic liquids and natural deep eutectic solvents,” *Journal of Molecular Liquids* 277, 932-958. DOI: 10.1016/j.molliq.2019.01.002

Fan, C., Liu, Y., Sebbah, T., and Cao, X. (2021). “A theoretical study on terpene-based natural deep eutectic solvent: Relationship between viscosity and hydrogen-bonding interactions,” *Global Challenges* 5(3), article ID 2000103. DOI: 10.1002/gch2.202000103

Florindo, C., Lima, F., Ribeiro, B. D., and Marrucho, I. M. (2019). “Deep eutectic solvents: Overcoming 21st century challenges,” *Current Opinion in Green and Sustainable Chemistry* 18, 31-36. DOI: 10.1016/j.cogsc.2018.12.003

Francisco, M., van den Bruinhorst, A., and Kroon, M. C. (2012). “New natural and renewable low transition temperature mixtures (LTTMs): Screening as solvents for lignocellulosic biomass processing,” *Green Chemistry* 14(8), 2153-2157. DOI: 10.1039/c2gc35660k

Gutiérrez, M. C., Rubio, F., and del Monte, F. (2010). “Resorcinol-formaldehyde polycondensation in deep eutectic solvents for the preparation of carbons and carbon - Carbon nanotube composites,” *Chemistry of Materials* 22(9), 2711-2719. DOI: 10.1021/cm9023502

Han, Q., Gao, X., Zhang, H., Chen, K., Peng, L., and Jia, Q. (2019). “Preparation and comparative assessment of regenerated cellulose films from corn (*Zea mays*) stalk pulp fines in DMAc/LiCl solution,” *Carbohydrate Polymers* 218, 315-323. DOI: 10.1016/j.carbpol.2019.04.083

Koprivica, S., Siller, M., Hosoya, T., Roggenstein, W., Rosenau, T., and Potthast, A. (2016). “Regeneration of aqueous periodate solutions by ozone treatment: A sustainable approach for dialdehyde cellulose production,” *ChemSusChem* 9(8), 825-833. DOI: 10.1002/cssc.201501639

Larsson, P. A., and Wågberg, L. (2016). “Towards natural-fibre-based thermoplastic films produced by conventional papermaking,” *Green Chemistry* 18(11), 3324-3333. DOI: 10.1039/C5GC03068D

Li, R., Wang, S., Lu, A., and Zhang, L. (2015). “Dissolution of cellulose from different sources in an NaOH/urea aqueous system at low temperature,” *Cellulose* 22(1), 339-349. DOI: 10.1007/s10570-014-0542-6

Lopez-Sanchez, P., Martinez-Sanz, M., Bonilla, M. R., Wang, D., Gilbert, E. P., Stokes, J. R., and Gidley, M. J. (2017). “Cellulose-pectin composite hydrogels: Intermolecular interactions and material properties depend on order of assembly,” *Carbohydrate Polymers* 162, 71-81. DOI: 10.1016/j.carbpol.2017.01.049

Lu, F., Wang, L., Zhang, C., Cheng, B., Liu, R., and Huang, Y. (2015). “Influence of temperature on the solution rheology of cellulose in 1-ethyl-3-methylimidazolium chloride/dimethyl sulfoxide," *Cellulose* 22(5), 3077-3087. DOI: 10.1007/s10570-015-0740-x

Lucia, A., Herwijnen. H., Oberlerchner. J. T. , Rosenau, P. T., Beaumont, M. (2019). "Resource-saving production of dialdehyde cellulose: Optimization of the process at high pulp consistency," *ChemSusChem* 12(20), 4679-4684. DOI: 10.1002/cssc.201901885

Luo, Y., Ma, H., Zhang, S., Zheng, D., Che, P., Liu, X., Zhang, M., Gao, J., and Xu, J. (2020). "Binding energy as driving force for controllable reconstruction of hydrogen bonds with molecular scissors," *Journal of the American Chemical Society* 142(13), 6085-6092. DOI: 10.1021/jacs.9b12117

Malaeke, H., Housaindokht, M. R., Monhemi, H., and Izadyar, M. (2018). "Deep eutectic solvent as an efficient molecular liquid for lignin solubilization and wood delignification," *Journal of Molecular Liquids* 263, 193-199. DOI: 10.1016/j.molliq.2018.05.001

Mamilla, J. L. K., Novak, U., Grilc, M., and Likozar, B. (2019). "Natural deep eutectic solvents (DES) for fractionation of waste lignocellulosic biomass and its cascade conversion to value-added bio-based chemicals," *Biomass and Bioenergy* 120, 417-425. DOI: 10.1016/j.biombioe.2018.12.002

Oh, S. Y., Yoo, D. I., Shin, Y., and Seo, G. (2005). "FTIR analysis of cellulose treated with sodium hydroxide and carbon dioxide," *Carbohydrate Research* 340(3), 417-428. DOI: 10.1016/j.carres.2004.11.027

Orelma, H., Korpela, A., Kunnari, V., Harlin, A., and Suurnäkki, A. (2017). "Improving the mechanical properties of CNF films by NMMO partial dissolution with hot calender activation," *Cellulose* 24(4), 1691-1704. DOI: 10.1007/s10570-017-1229-6

Ren, H., Chen, C., Wang, Q., Zhao, D., and Guo, S. (2016). "The properties of choline chloride-based deep eutectic solvents and their performance in the dissolution of cellulose," *BioResources* 11(2), 5435-5451. DOI: 10.15376/biores.11.2.5435-5451

Sirviö, J., Hyvakko, U., Liimatainen, H., Niinimaki, J., and Hormi, O. (2011a). "Periodate oxidation of cellulose at elevated temperatures using metal salts as cellulose activators," *Carbohydrate Polymers* 83(3), 1293-1297. DOI: 10.1016/j.carbpol.2010.09.036

Sirviö, J., Liimatainen, H., Niinimäki, J., and Hormi, O. (2011b). "Dialdehyde cellulose microfibers generated from wood pulp by milling-induced periodate oxidation," *Carbohydrate Polymers* 86(1), 260-265. DOI: 10.1016/j.carbpol.2011.04.054

Sosa, F. H. B., Abranches, D. O., da Costa Lopes, A. M., Coutinho, J. A. P., and da Costa, M. C. (2020). "Kraft lignin solubility and its chemical modification in deep eutectic solvents," *ACS Sustainable Chemistry and Engineering* 8(50), 18577-18589. DOI: 10.1021/acssuschemeng.0c06655

Tang, X., Zuo, M., Li, Z., Liu, H., Xiong, C., Zeng, X., Sun, Y., Hu, L., Liu, S., Lei, T., *et al.* (2017). "Green processing of lignocellulosic biomass and its derivatives in deep eutectic solvents," *ChemSusChem* 10(13), 2696-2706. DOI: 10.1002/cssc.201700457

Xiao, P., Zhang, J., Feng, Y., Wu, J., He, J., and Zhang, J. (2014). "Synthesis, characterization and properties of novel cellulose derivatives containing phosphorus: Cellulose diphenyl phosphate and its mixed esters," *Cellulose* 21(4), 2369-2378. DOI: 10.1007/s10570-014-0256-9

Xu, Y., Guo, L., Zhang, H., Zhai, H., and Ren, H. (2019). "Research status, industrial application demand and prospects of phenolic resin," *RSC Advances* 9(50), 28924-28935. DOI: 10.1039/c9ra06487g

Yue, X., Suopajärvi, T., Mankinen, O., Mikola, M., Mikkelson, A., Ahola, J., Hiltunen, S., Komulainen, S., Kantola, A. M., Telkki, V., *et al.* (2020). "Comparison of lignin fractions isolated from wheat straw using alkaline and acidic deep eutectic solvents," *Journal of Agricultural and Food Chemistry* 68(51), 15074-15084. DOI: 10.1021/acs.jafc.0c04981

Zhang, H., Lang, J., Lan, P., Yang, H., Lu, J., and Wang, Z. (2020). "Study on the dissolution mechanism of cellulose by ChCl-based deep eutectic solvents," *Materials* 13(2), Article Number 278. DOI: 10.3390/ma13020278

Zhou, E., and Liu, H. (2014). "A novel deep eutectic solvents synthesized by solid organic compounds and its application on dissolution for cellulose," *Asian Journal of Chemistry* 26(12), 3626-3630. DOI: 10.14233/ajchem.2014.16995

Article submitted: January 23, 2022; Peer review completed: April 30, 2022; Revised version received and accepted: May 14, 2022; Published: May 19, 2022.
DOI: 10.15376/biores.17.3.4167-4185

APPENDIX

Supplementary Data: Molecular Simulation Details

The hydrogen bond network of DES and dissolved samples was investigated by molecular dynamics simulation using package Materials Studio 2017 developed by Accelrys Incorporation (Cambridge, UK). Resorcinol and choline chloride models were built and their electron density pattern was analyzed using Dmol3 module. DES comprising of 73 ChCl molecules and 73 resorcinol molecules was established using Amorphous Cell module. Energy optimization and geometry optimization were performed using Dmol3 module. The type and number of hydrogen bonds in DES are summarized in Table S1.

Table S1. Hydrogen Bonding Statistics in DES

	H_{Ch}	H_{RES}
Cl^{-}	42	67
O_{Ch}	3	11
O_{RES}	14	25

The cellulose chain (5 anhydroglucose units) was used to build the PAC model with 20% of reaction level. Then, PAC structure was optimized using Forcite module. Two PAC molecules and DES were mixed to establish dissolved samples model using Amorphous Cell module. In this dissolved samples model, the weight ratio of PAC to DES was approximately 12%. Energy optimization, geometry optimization, annealing treatment, and dynamic optimization of dissolved samples were performed in the Forcite module. The type and number of hydrogen bonds in dissolved samples are summarized in Table S2.

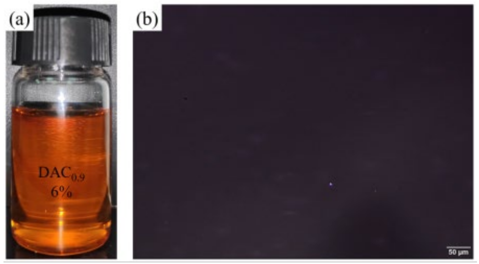

Fig. S1. (a) The dissolved samples of DAC in DES, the weight ratio of periodate to MCC was 0.9, corresponding to the oxidation level of 25.6%, (b) the POM images of dissolved samples. The cellulose crystalline is hardly observed in this POM image, which proved that DAC can almost entirely dissolve in DES at a higher oxidation level.

Table S2. Hydrogen Bonding Statistics in DES/DAC Dissolved System

	H_{Ch}	H_{RES}	H_{PAC}
Cl^{-}	41	86	20
O_{Ch}	5	12	2
O_{RES}	16	33	2
O_{PAC}	4	5	14